Supporting Information

Efficient Solar Cells with Enhanced Humidity and Heat Stability Based on Benzylammonium-caesium-formamidinium Mixed-Dimensional Perovskites

Guozhen Liu,[ab] Haiying Zheng,[ab] Xiaoxiao Xu,[ab] Liangzheng Zhu,[ab] Ahmed Alsaedi,[c] Tasawar Hayat,[ce] Xu Pan*[a] and Songyuan Dai*[acd]

[a]Key Laboratory of Photovoltaic and Energy Conservation Materials, Institute of Applied Technology, Hefei Institutes of Physical Science, Chinese Academy of Sciences, Hefei 230031, China.

[b]University of Science and Technology of China, Hefei 230026, China.

[c]NAAM Research Group, Department of Mathematics, Faculty of Science, King Abdulaziz University, Jeddah 21589, Saudi Arabia.

[d]State Key Laboratory of Alternate Electrical Power System with Renewable Energy Sources, North China Electric Power University, Beijing 102206, China.

[e]Department of Mathematics, Quaid-I-Azam University, Islamabad 44000, Pakistan.

*Email: xpan@rntek.cas.cn

Experimental Section

Preparation of perovskite precursor

$HC(NH_2)_2I$ (FAI) and $HC(NH_2)_2Br$ (FABr) synthesis: FAI and FABr were prepared by dissolving formamidine acetate (98%, Sinopharm) in the excess of hydroiodic acid (HI, 57 wt% in H_2O, sigma-aldrich) and hydrobromic acid (HBr, 47 wt% in H_2O, sigma-aldrich) in a flask, respectively. After addition of HI or HBr, the solution was stirred at 0 °C for about 2 h. By rotary evaporation for 2 h at 60 °C, two white powders were obtained, respectively. After drying, the powders were recrystallized in diethyl ether. Finally, the purified FAI and FABr were gained by drying in a vacuum oven at 60 °C.

$C_6H_5CH_2NH_3I$ (BEI) synthesis: BEI was obtained by reacting hydroiodic acid (HI, 57 wt%) with benzylamine (BE, 98.5%, Sinopharm) for about 1 h, the other preparation steps were same as the above.

Preparation of MD perovskite precursor solution: The $[(BE_2PbI_4)_x(FA_{0.9}Cs_{0.1}PbI_3)_{1-x}]_{0.85}(FAPbBr_3)_{0.15}$ precursor solutions (1.35 M Pb^{2+}) were obtained by dissolving corresponding lead iodide (PbI_2, TCI), lead bromide ($PbBr_2$, TCI), FAI, FABr, BEI and caesium iodide (CsI, Alfa) in mixed solvent of anhydrous methyl sulfoxide (DMSO, Sinopharm) and anhydrous N,N-dimethylformamide (DMF, Sinopharm) (DMSO:DMF=1:4 by volume) with stoichiometrically. $MAPbI_3$ perovskite solution (1.35 M Pb^{2+}) was composed of corresponding lead iodide (PbI_2, TCI) and methylammonium iodide CH_3NH_3I (MAI, ≥99.5%, Xi'an p-OLED Corp.) in mixed solvent of anhydrous methyl sulfoxide (DMSO, Sinopharm) and anhydrous N, N-dimethylformamide (DMF, Sinopharm) (DMSO: DMF=4:1 by volume). Then, all the solutions were stirred for 1 h at 65 °C and filtered using 0.45 µm PVDF filters before film deposition.

Device fabrication: All of the perovskite devices were deposited on pretreated FTO substrate. The compact layer of TiO_2 was coated by a spray pyrolysis method at 430 °C. The solution was gained by mixing the bis(acetylacetonate) (0.4 mL, Sinopharm, 99%) and titanium diisopropoxide (0.6 mL, Aldrich, 97%) in anhydrous isopropanol (7 mL, Sinopharm, 99.7%). Then, the mesoporous layer of TiO_2 was deposited by spin-coating the TiO_2 paste (30 nm, Dyesol, TiO_2: anhydrous ethanol =1:5.5 by weight) at 4000 r.p.m for 20 s and heated at 500 °C for 30 min. The perovskite layers were spin-coated on the mesoporous layer in the glovebox at 1100 r.p.m for 10 s and 4600 r.p.m for 35 s. Chlorobenzene (120 µL) was drop-added on the surface during the spin coating step 15 s before the end. Then, the substrate should be annealed for 50 min at 105 °C. The HTM solution, composing of 73-mg spiro-OMeTAD, 29-µL 4-tert-butylpyridine, 17-µL Li^+ salt and 8-µL cobalt(III) salt in 1-mL chlorobenzene, was then spin-coated on the perovskite at 3000 r.p.m for 20 s. Finally, about 65-nm Au electrode was thermally evaporated under high vacuum.

Characterizations: XRD patterns were characterized using a Smartlab 9KW with the 2θ range from 5° to 50°. SEM images were recorded on a high-resolution field-emission scanning electron microscope (FE-SEM, sirion200, FEI Corp., Holland). Ultraviolet-visible absorption spectra were characterized by ultraviolet−vis (UV−vis) spectrophotometer (U-3900H, HITACHI, Japan) with the measurement from 300 nm to 900 nm. Steady-state Photoluminescence (PL) spectra were measured by the spectrofluorometer (photon technology international). They were analyzed by a software Fluorescence. The samples were excited with a standard 450 W xenon CW lamp with an exciting wavelength of 473 nm. *J–V* curves were measured by a solar simulator (Newport, Oriel Class A, 91195A) at 100 mW/cm^2 illumination AM 1.5G with an active area of 0.09 cm^2. The scan rate is 50 $mV\ s^{-1}$. The source meter is Keithley 2420. Incident photon to current conversion efficiency (IPCE) spectra (300 nm to 900 nm) were executed on dual Xenon/quartz halogen light source (PV

Measurements, Inc.) in DC mode without bias light. Transient absorption (TA) were performed by the spectra LKS (Applied photophysics). The laser energy was 150 μJ/cm^2 with a repetition rate of 5 Hz. The samples were tested under a 760-nm probe light wavelength and a 500-nm laser light wavelength. The construction of sample is glass/perovskite film.

Stability test: The perovskite devices were placed in a containers with 50±5% RH to measure the humidity stability at room temperature in dark. Heat stability measurement was executed in a container at 85 °C in dark. All perovskite devices were aged under the same conditions.

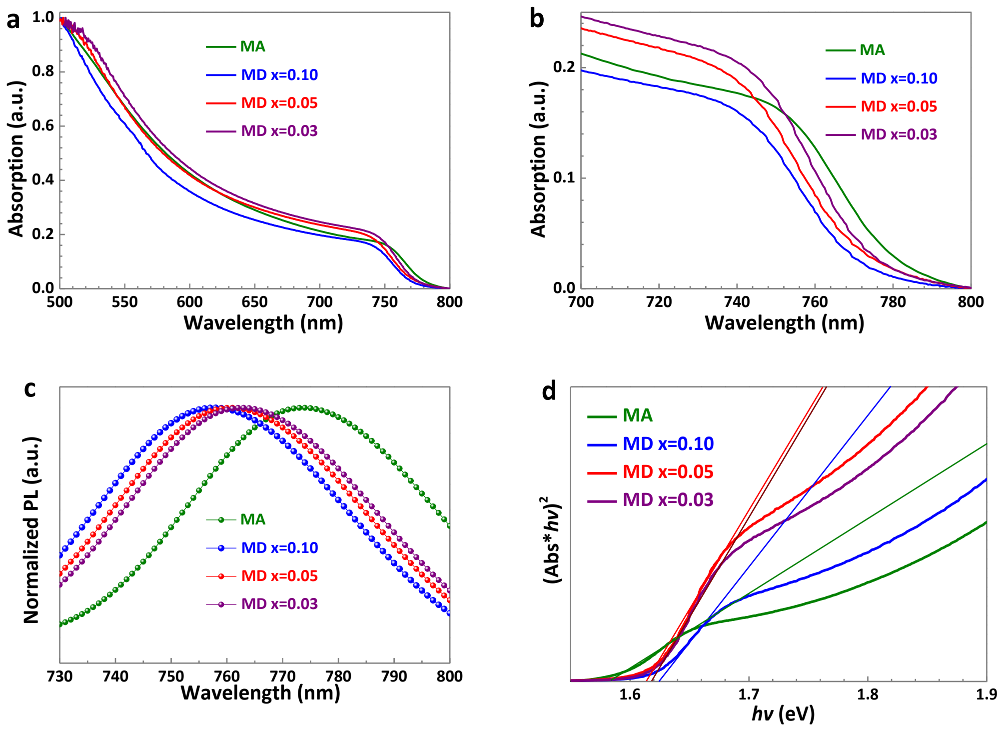

Fig. S1. (a) Normalized UV-vis absorption spectra, (b) partially enlarged normalized UV-vis absorption spectra and (c) partially enlarged normalized PL spectra of $MAPbI_3$ and $[(BE_2PbI_4)_x(FA_{0.9}Cs_{0.1}PbI_3)_{1-x}]_{0.85}(FAPbBr_3)_{0.15}$ (x=0.03, 0.05, 0.10) thin films. (d) Tauc plot from the UV-vis spectra of $MAPbI_3$ and $[(BE_2PbI_4)_x(FA_{0.9}Cs_{0.1}PbI_3)_{1-x}]_{0.85}(FAPbBr_3)_{0.15}$ (x=0.03, 0.05, 0.10) films.

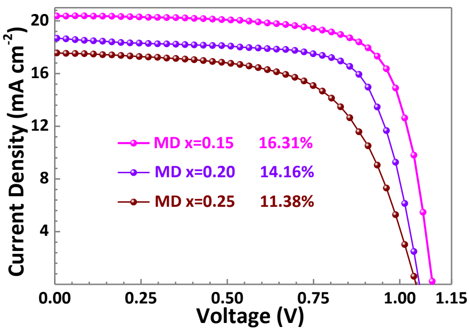

Fig. S2. *J−V* curves of $[(BE_2PbI_4)_x(FA_{0.9}Cs_{0.1}PbI_3)_{1-x}]_{0.85}(FAPbBr_3)_{0.15}$ (x=0.15, 0.20, 0.25) PSCs.

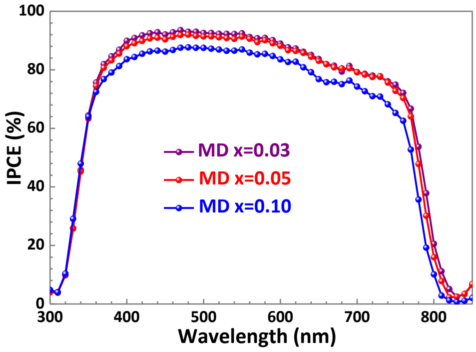

Fig. S3. IPCE spectra of the MD (x=0.03, 0.05 and 0.10) perovskite devices.

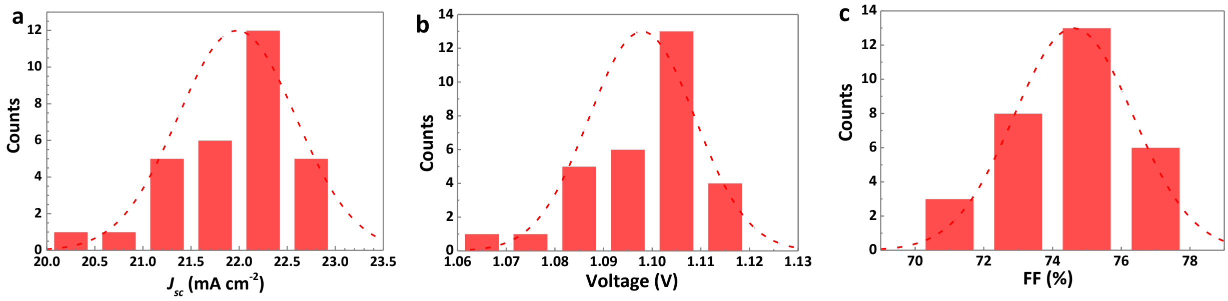

Fig. S4. (a) Short-circuit current density (J_{sc}), (b) Open circuit voltages (V_{oc}) and (c) Fill factor (FF) histogram fitted with a Gaussian distribution of the MD (x=0.05) perovskite devices over 30 measured devices.

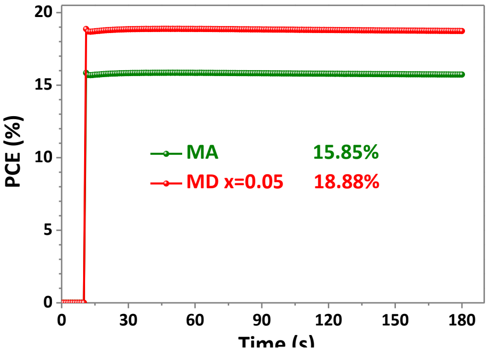

Fig. S5. Stabilized power output at maximum power point as a function of time for the best performing $MAPbI_3$ and MD (x=0.05) devices.

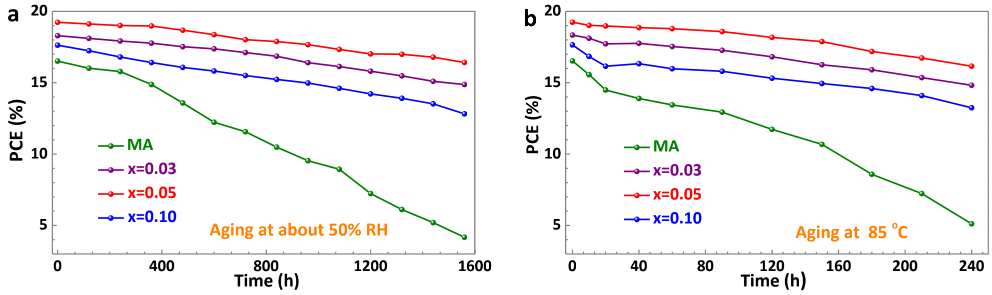

Fig. S6. PCE variation curves of unsealed $MAPbI_3$ and $[(BE_2PbI_4)_x(FA_{0.9}Cs_{0.1}PbI_3)_{1-x}]_{0.85}(FAPbBr_3)_{0.15}$ (x=0.03, 0.05, 0.10) perovskite devices when exposing to (a) 50% RH for 1600 h and (b) 85 °C for 240 h.

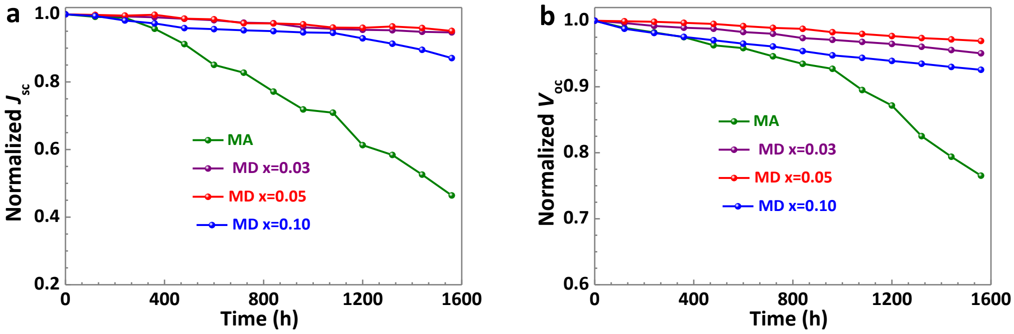

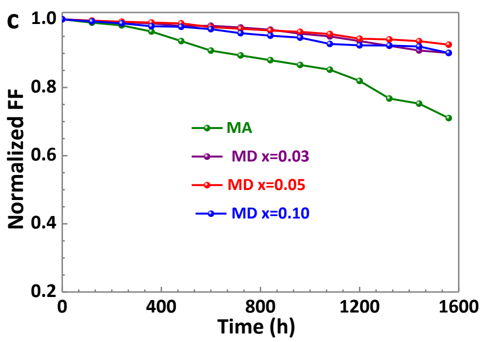

Fig. S7. Normalized (a) short-circuit current density (J_{sc}), (b) open circuit voltages (V_{oc}) and (c) fill factor (FF) variation curves of unsealed $MAPbI_3$ and $[(BE_2PbI_4)_x(FA_{0.9}Cs_{0.1}PbI_3)_{1-x}]_{0.85}(FAPbBr_3)_{0.15}$ (x=0.03, 0.05, 0.10) perovskite devices under about 50% RH.

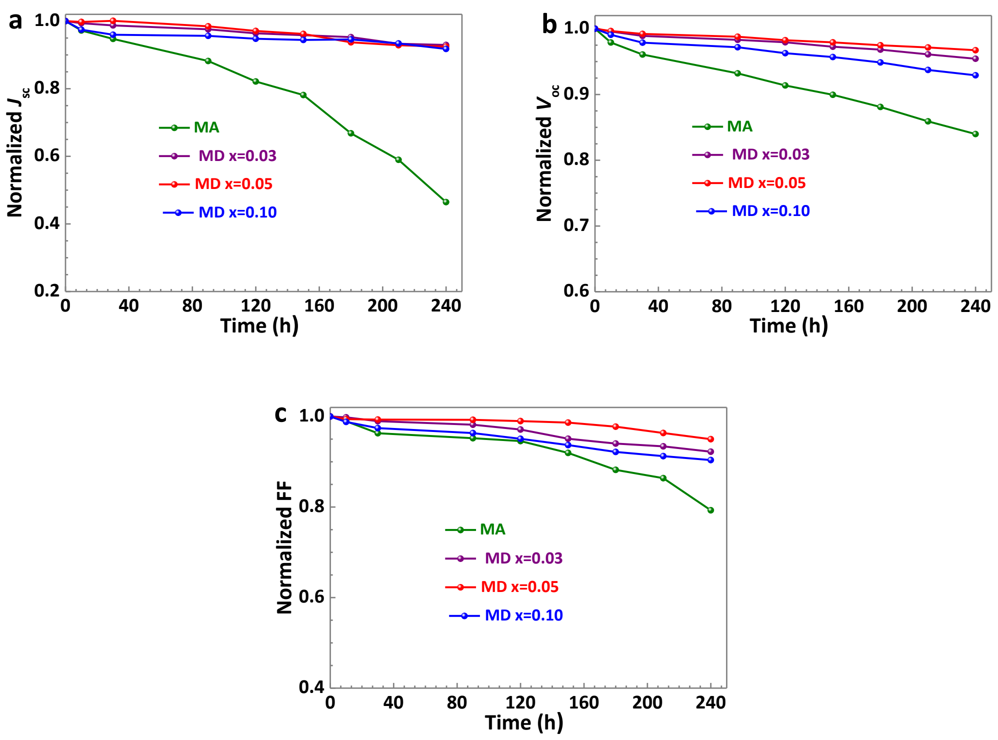

Fig. S8. Normalized (a) short-circuit current density (J_{sc}), (b) open circuit voltages (V_{oc}) and (c) fill factor (FF) variation curves of unsealed $MAPbI_3$ and $[(BE_2PbI_4)_x(FA_{0.9}Cs_{0.1}PbI_3)_{1-x}]_{0.85}(FAPbBr_3)_{0.15}$ (x=0.03, 0.05, 0.10) perovskite devices at 85 °C.

Table S1. Photovoltaic parameters of the $MAPbI_3$ and the MD (x=0.05) perovskite devices under reverse and forward scan directions.

Device	J_{sc} (mA cm^{-2})	V_{oc} (V)	FF (%)	PCE (%)
MA-Reverse	21.49	1.07	71.67	16.53
MA-Forward	20.18	1.07	68.74	14.86
MD-Reverse	22.79	1.10	76.74	19.24
MD-Forward	22.38	1.10	75.80	18.69

Table S2. Photovoltaic parameters of $[(BE_2PbI_4)_x(FA_{0.9}Cs_{0.1}PbI_3)_{1-x}]_{0.85}(FAPbBr_3)_{0.15}$ (x=0.15, 0.20, 0.25) PSCs.

Device	J_{sc} (mA cm^{-2})	V_{oc} (V)	FF (%)	PCE (%)
x=0.15	20.38	1.10	73.07	16.31
x=0.20	18.69	1.06	71.67	14.16
x=0.25	17.55	1.05	61.94	11.38

Table S3. Photovoltaic parameters of $[(BE_2PbI_4)_x(FA_{0.9}Cs_{0.1}PbI_3)_{1-x}]_{0.85}(FAPbBr_3)_{0.15}$ (x=0.15, 0.20, 0.25) PSCs for humidity stability measurements under about 50% RH.

$MAPbI_3$	J_{sc} (mA cm^{-2})	V_{oc} (V)	FF (%)	PCE (%)
0 h	21.49	1.07	71.67	16.51
120 h	21.33	1.06	70.96	16.02

240 h	21.27	1.05	70.39	15.79
360 h	20.57	1.05	69.09	14.87
480 h	19.59	1.03	67.09	13.58
600 h	18.27	1.03	65.08	12.23
720 h	17.78	1.02	64.08	11.57
840 h	16.58	1.00	63.08	10.49
960 h	15.44	0.99	62.07	9.53
1080 h	15.23	0.96	61.07	8.94
1200 h	13.17	0.93	58.70	7.23
1320 h	12.55	0.89	55.01	6.11
1440 h	11.30	0.85	53.94	5.19
1560 h	9.97	0.82	50.90	4.17

MD (x=0.03)	J_{sc} (mA cm^{-2})	V_{oc} (V)	FF (%)	PCE (%)
0 h	22.83	1.09	73.63	18.30
120 h	22.74	1.09	73.27	18.11
240 h	22.68	1.08	72.99	17.92
360 h	22.62	1.08	72.77	17.77
480 h	22.52	1.08	72.18	17.52
600 h	22.43	1.07	72.23	17.37

720 h	22.26	1.07	71.87	17.12
840 h	22.22	1.06	71.39	16.86
960 h	21.95	1.06	70.53	16.40
1080 h	21.85	1.06	69.94	16.14
1200 h	21.78	1.05	68.92	15.81
1320 h	21.75	1.05	67.91	15.48
1440 h	21.64	1.04	66.89	15.10
1560 h	21.61	1.04	66.37	14.87

MD (x=0.05)	J_{sc} (mA cm^{-2})	V_{oc} (V)	FF (%)	PCE (%)
0 h	22.77	1.10	76.74	19.23
120 h	22.73	1.10	76.44	19.12
240 h	22.68	1.10	76.20	19.01
360 h	22.74	1.10	76.01	18.98
480 h	22.48	1.10	75.82	18.68
600 h	22.43	1.09	74.98	18.37
720 h	22.17	1.09	74.61	18.02
840 h	22.16	1.09	74.22	17.89
960 h	22.10	1.08	73.91	17.67
1080 h	21.88	1.08	73.42	17.33

1200 h	21.86	1.08	72.38	17.02
1320 h	21.95	1.07	72.20	16.99
1440 h	21.85	1.07	71.82	16.79
1560 h	21.65	1.07	71.02	16.42

MD (x=0.10)	J_{sc} (mA cm^{-2})	V_{oc} (V)	FF (%)	PCE (%)
0 h	21.71	1.12	72.57	17.63
120 h	21.61	1.11	72.12	17.24
240 h	21.32	1.10	71.71	16.80
360 h	21.13	1.09	71.10	16.41
480 h	20.83	1.09	70.98	16.07
600 h	20.76	1.08	70.47	15.82
720 h	20.68	1.08	69.62	15.50
840 h	20.63	1.07	69.09	15.23
960 h	20.55	1.06	68.67	14.98
1080 h	20.52	1.06	67.33	14.61
1200 h	20.17	1.05	67.02	14.22
1320 h	19.82	1.05	66.99	13.91
1440 h	19.43	1.04	66.79	13.52
1560 h	18.90	1.04	65.42	12.82

Table S4. Photovoltaic parameters of $[(BE_2PbI_4)_x(FA_{0.9}Cs_{0.1}PbI_3)_{1-x}]_{0.85}(FAPbBr_3)_{0.15}$ (x=0.15, 0.20, 0.25) PSCs for heat stability measurements 85 °C.

$MAPbI_3$	J_{sc} (mA cm^{-2})	V_{oc} (V)	FF (%)	PCE (%)
0	21.48	1.07	71.67	16.53
10	20.89	1.05	70.92	15.57
20	20.35	1.03	69.02	14.49
40	19.77	1.02	68.89	13.89
60	19.39	1.01	68.56	13.44
90	18.95	1.00	68.23	12.94
120	17.64	0.98	67.78	11.73
150	16.78	0.97	65.91	10.68
180	14.35	0.95	63.22	8.58
210	12.67	0.92	61.91	7.23
240	9.98	0.90	56.82	5.11

MD (x=0.03)	J_{sc} (mA cm^{-2})	V_{oc} (V)	FF (%)	PCE (%)
0	22.83	1.09	73.63	18.34
10	22.67	1.09	73.50	18.12
20	22.53	1.08	72.87	17.72
40	22.64	1.08	72.61	17.76

60	22.41	1.07	72.37	17.54
90	22.27	1.07	72.29	17.27
120	22.00	1.07	71.51	16.81
150	21.87	1.06	70.02	16.26
180	21.74	1.06	69.23	15.90
210	21.29	1.05	68.77	15.36
240	21.22	1.04	67.90	14.82

MD (x=0.05)	J_{sc} (mA cm^{-2})	V_{oc} (V)	FF (%)	PCE (%)
0	22.77	1.10	76.74	19.24
10	22.72	1.10	76.29	19.02
20	22.79	1.09	76.21	18.98
40	22.70	1.09	76.22	18.86
60	22.62	1.09	76.20	18.79
90	22.42	1.09	76.18	18.58
120	22.11	1.08	75.97	18.18
150	21.91	1.08	75.70	17.89
180	21.34	1.07	75.01	17.19
210	21.15	1.07	73.94	16.73
240	21.05	1.07	72.89	16.16

MD (x=0.10)	J_{sc} (mA cm^{-2})	V_{oc} (V)	FF (%)	PCE (%)
0	21.71	1.12	72.57	17.65
10	21.16	1.11	71.70	16.84
20	20.83	1.10	70.71	16.16
40	21.14	1.09	70.84	16.33
60	20.92	1.09	70.09	15.98
90	20.76	1.09	69.91	15.80
120	20.58	1.08	68.99	15.31
150	20.50	1.07	67.99	14.94
180	20.53	1.06	66.89	14.60
210	20.28	1.05	66.21	14.10
240	19.92	1.04	65.58	13.25